

Surgical Management of Chiari Malformation Type I and Instability of the Craniocervical Junction Based on Its Pathogenesis and Classification

Misao NISHIKAWA,¹ Paolo A. BOLOGNESE,² Toru YAMAGATA,¹ Kentarou NAITO,³
Hiroaki SAKAMOTO,⁴ Mistuhiro HARA,¹ Kenji OHATA,⁵ and Takeo GOTO³

¹Department of Neurosurgery, Moriguchi-Ikuno Memorial Hospital, Moriguchi, Osaka, Japan

²Department of Neurosurgery, Chiari Ehlas Danlos Syndrome Center, Mount Sinai South Nassau, Lake Success, Nassau, New York, USA

³Department of Neurosurgery, Osaka Metropolitan University Graduate School of Medicine, Osaka, Osaka, Japan

⁴Department of Pediatric Neurosurgery, Osaka City General Hospital, Osaka, Osaka, Japan

⁵Department of Neurosurgery, Naniwa-Ikuno Hospital, Osaka, Osaka, Japan

Abstract

We investigated the mechanism underlying Chiari malformation type I (CM-I) and classified it according to the morphometric analyses of posterior cranial fossa (PCF) and craniocervical junction (CCJ). Three independent subtypes of CM-I were confirmed (CM-I types A, B, and C) for 484 cases and 150 normal volunteers by multiple analyses. CM-I type A had normal volume of PCF (VPCF) and occipital bone size. Type B had normal VPCF and small volume of the area surrounding the foramen magnum (VAFM) and occipital bone size. Type C had small VPCF, VAFM, and occipital bone size. Morphometric analyses during craniocervical traction test demonstrated instability of CCJ. Foramen magnum decompression (FMD) was performed in 302 cases. Expansive suboccipital cranioplasty (ESCP) was performed in 102 cases. Craniocervical posterolateral fixation (CCF) was performed for CCJ instability in 70 cases. Both ESCP and FMD showed a high improvement rate of neurological symptoms and signs (84.4%) and a high recovery rate of the Japanese Orthopaedic Association (JOA) score (58.5%). CCF also showed a high recovery rate of the JOA score (69.7%), with successful joint stabilization (84.3%). CM-I type A was associated with other mechanisms that caused ptosis of the brainstem and cerebellum (CCJ instability and traction and pressure dissociation between the intracranial cavity and spinal canal cavity), whereas CM-I types B and C demonstrated underdevelopment of the occipital bone. For CM-I types B and C, PCF decompression should be performed, whereas for small VPCF, ESCP should be performed. CCF for CCJ instability (including CM-I type A) was safe and effective.

Keywords: Chiari malformation, craniocervical junction, instability, pathogenesis, surgical intervention

Background and Purpose

Previously, we reported that patients with Chiari malformation type I (CM-I) have an underdeveloped occipital bone, which leads to a shallow posterior cranial fossa (PCF).¹⁻³⁾ The shallow PCF causes sagging of the brainstem and cerebellum into the spinal canal, similar to ptosis. A

number of reports have provided support for our hypothesis and the underlying pathogenic mechanism.⁴⁻⁸⁾ In addition, developmental biological studies provided further support by demonstrating the presence of genetic abnormalities that influence the segmentation of the paraxial mesoderm.^{2,9-11)} Other mechanisms causing ptosis of the brainstem and cerebellum include instability of the cranio-

Received March 16, 2022; Accepted June 14, 2022

Copyright © 2022 The Japan Neurosurgical Society

This work is licensed under a Creative Commons Attribution-NonCommercial-NoDerivatives International License.

cervical junction (CCJ) and traction due to tethering.^{12,13)} The unclear mechanism underlying ptosis of the brainstem and cerebellum in CM-I has resulted in the inappropriate selection of surgical treatment. Therefore, it is necessary to reappraise and classify CM-I. However, a diagnostic strategy that clearly demonstrates the mechanism underlying ptosis of the brainstem and cerebellum has not been developed.

The appropriate choice of surgical treatment for CCJ instability, which is not rare and results in severe symptoms, is also of clinical interest. However, a diagnostic strategy for CCJ instability has not been developed. The lack of clarity of the mechanisms underlying joint instability and its effects has resulted in the selection of inappropriate surgical treatment.

Since 2006, we have been performing morphometric studies for PCF and CCJ during craniocervical traction test—an approach that we designed and established. We have conducted multiple analyses of this strategy in cases with CM-I. In the present study, we examined the mechanism underlying ptosis of the brainstem and cerebellum using morphometric analysis to redefine and classify CM-I. We also discuss the surgical treatment approaches for the mechanism underlying ptosis of the brainstem and cerebellum. We also present the preliminary results of the treatments for ptosis of the brainstem and cerebellum in cases with CM-I. In addition, we present the preliminary results of the interventions for CCJ instability.

Volumetric and Morphometric Analyses of PCF and CCJ (Figs. 1 and 2)

I. Materials

1. Normal controls and inclusion criteria

This study recruited 150 normal volunteers (controls) with no neurological symptoms or abnormalities in the neural axis (aged 4–49 years, mean: 18.7 years, 64 males and 86 females). In addition, 447 patients with CM-I (cerebellar tonsil herniation ≥ 5 mm from the McRae line, i.e., between the basion and opisthion), presence of brainstem symptoms, and/or myelopathy (aged 4–49 years, mean: 18.1 years, 199 males and 248 females), as well as 37 patients with CM-borderline (cerebellar tonsil herniation < 5 mm from the McRae line, but presence of brainstem symptoms and/or myelopathy) (aged 5–45 years, mean: 18.4 years, 15 males and 22 females), were included. Age and sex were not significantly different between the normal controls and CM-I group.

The patients were diagnosed and treated between April 2002 and March 2020. The normal controls and patients had various Asian ethnicities (Asian American, Asian European, Chinese, Korean, and Japanese), considering ethnic variation.^{14,15)} The normal controls and patients were managed at The Chiari Institute North Shore University Hospital (NY, USA), Moriguchi-Ikuno Memorial Hospital, Osaka

Metropolitan University Hospital, and Osaka City General Hospital.

2. Exclusion criteria

We excluded cases with myelopathy and/or radiculopathy due to disc herniation, spondylotic changes, and ossification of the longitudinal ligament. In addition, we excluded patients 50 or older than 50 years because of age-related changes in the brain and degeneration of the bony structures. Infants and toddlers younger than 4 years were excluded because of the rapid development and growth, and the risk of radiation in this age group.

3. Associated conditions

CM-I and CM-borderline were associated with syringomyelia in 248 cases (51.2%), hereditary disorders of connective tissue (HDCT) in 30 cases (6.2%), basilar invagination in 28 cases (5.8%), other bony anomalies (e.g., assimilation of the atlas, platybasia, and os odontoideum) in CCJ in 57 (11.8%) cases, tethered cord syndrome in 25 cases (5.2%), syndrome of hypotension of cerebrospinal fluid (CSF) pressure in 22 cases (4.5%), hydrocephalus in 12 cases (2.5%), and intracranial mass lesion in 10 cases (2.1%).

II. Methods

1. Volumetric and morphometric analyses of PCF, brainstem, and cerebellum (Fig. 1 and 2-1A-C)

We used 2D- or 3D-CT reconstructed images using Osirix software (freely available) to calculate the volume of PCF (VPCF) (Fig. 1A and B), volume of the surrounding area of the foramen magnum (VAFM, i.e., total volume between the inferior and superior outlets of the foramen magnum) (Fig. 1C and D).¹⁻³⁾ VPCF was divided into the volume of the area of the PCF above and below the Twining's line (VPCF-ATW and VPCF-BTW). The volume of the brain in the PCF (VBPCF) was calculated on magnetic resonance (MR) axial and sagittal images, excluding the 4th ventricle, herniated cerebellar tonsils, and medulla oblongata.

On 2D-CT coronal images at the occipital condyle and midline sagittal plane, the axial lengths of the basiocciput (clivus), exocciput (condyle), and supraocciput as enchondral parts of the occipital bone (occipital bone size) were measured (Fig. 2-1A and B). Using an MR midline image, the axial length of the brain stem (BSL), medullary height (MH), and the position of 4th ventricle (4VH) were measured (Fig. 2-1C).¹⁻³⁾

CM-I was categorized on the basis of multiple analyses. The radiographic analysis was performed using Osirix software.

2. Morphometric measurement and evaluation of CCJ instability (Fig. 2-2D-F)

CCJ instability was diagnosed using a morphometric

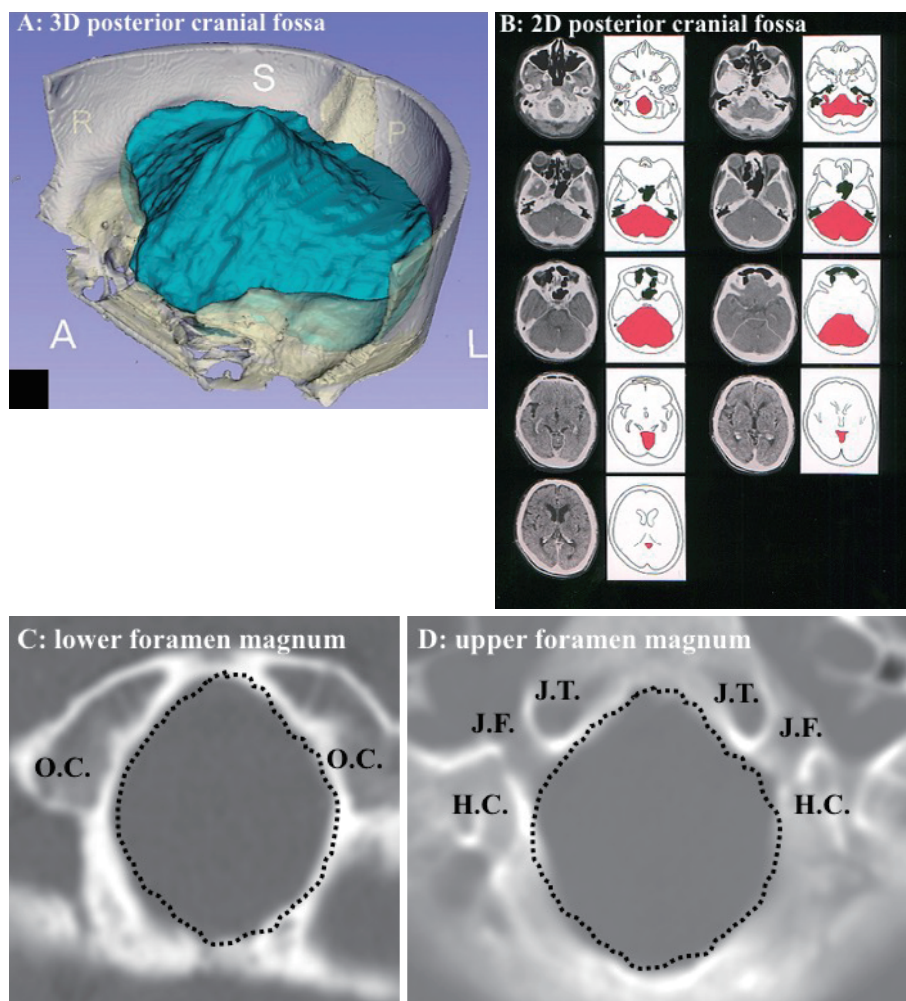


Fig. 1 Volumetric examination of the posterior cranial fossa (PCF).

A, B, C, and D were reproduced from [11] with permission.

A: 3D-CT reconstructed image of the PCF using Osirix software.

B: 2D-CT images of the PCF. Red areas indicate the volume of PCF (VPCF).

C: 2D-CT image demonstrating the area of the inferior outlet of the foramen magnum at the level of the basion and opisthion.

D: 2D-CT image demonstrating the area of the superior outlet of the foramen magnum at the level of the jugular tubercle.

The PCF was defined as the almost circular space bounded by the tentorium cerebelli, occipital bone, clivus, petrous bone, and petrous ridges. The ridges of the petrous bones form the anterolateral border of the cavity and their connection to the posterior clinoids (posterior petroclinoid ligament) forms the anterior border. The caudal end of PCF was defined as the foramen magnum, including the McRae's line. McRae's line was defined as the line between the basion and opisthion. The volume of brain in PCF (VBPCF) was calculated as the neural content of the PCF, including the cerebellum, mesencephalon, pons, and medulla (blue areas in A, and red areas in B).

Abbreviations: A = anterior, P = posterior, L = left, R = right, H.C. = hypoglossal nerve canal, J.F. = jugular foramen, J.T. = jugular tubercle, O.C. = occipital condyle

study and craniocervical traction test, which were described by the authors of the present study and Goel et al. in past reports and a textbook.^{12,16-20} For the craniocervical traction test, a tong was attached to the skull under intravenous anesthesia in the supine position and morphometric measurements were performed. Then, the patient was placed in an upright position and craniocervical instability was assessed on the basis of neurological symptoms, followed by repeat morphometric measurements. Cases with

displacement of the occipito-atlanto-axial joints (> 1.5 standard deviation [SD]) were defined as having instability. Craniocervical traction using 10-15 kg was applied, which resolved the neurological symptoms and led to a reduction of the occipito-atlanto-axial joints.

We did not perform CCJ traction test for individuals younger than 12 years, who are inside the growth period, to avoid inaccurate evaluation of instability and need for invasive intervention for the child during development and

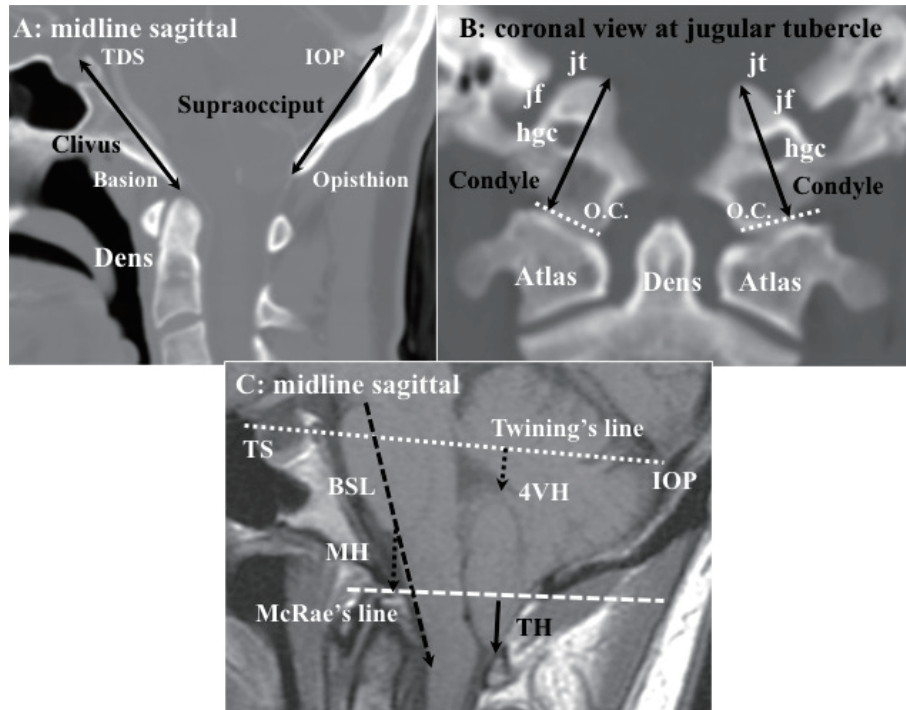


Fig. 2-1 Morphometric measurements of the posterior cranial fossa (PCF) and craniocervical junction (CCJ).

A, B, C, D, E, and F were reproduced from [11] with permission.

A: 2D-CT midline sagittal image demonstrating morphometric measurements of the basiocciput (clivus) (left black double arrow) and supraocciput (right black double arrow).

B: 2D-CT coronal image at the hypoglossal nerve canal (hgc) and jugular tubercle (jt) demonstrating morphometric measurements of the exocciput (condyle) (double black arrows). O.C. = articular process of the occipital condyle (white dotted lines).

C: Magnetic resonance (MR) midline sagittal image demonstrating morphometric measurements of the axial length of the brain-stem (BSL) (large black dotted line), medullary height (MH) (black small dotted line), and the position of the 4th ventricle (4VH) (black small dotted line).

Abbreviations: IOP = internal occipital protuberance, TDS = top of tuberculum sellae, Twining's line (white small dotted lines) = line between the tuberculum sellae (TS) and internal occipital protuberance (IOP), McRae's line = line between the basion and opisthion, TH = tonsillar herniation (black arrow)

The measurements included the axial length of the clivus (basiocciput and basisphenoid) from the top of the dorsum sellae to the basion; the axial length of the supraocciput from the center of the internal occipital protuberance to the opisthion; and the axial length of the occipital condyle (exocciput) from the top of the jugular tubercle to the bottom of the occipital condyle and the supraocciput (distance between the opisthion and the center of the internal occipital protuberance). These three measurements were combined as the occipital bone size. The axial length of the brain stem (BSL) was calculated between the midbrain-pons junction and medullo-cervical junction. MH was defined as the vertical distance between the ponto-medullary junction and McRae's line. The position of the 4th ventricle (4VH) was defined as the vertical distance between the fastigium (transverse summit of the roof of fourth ventricle) of the 4th ventricle and Twining's line. TH indicates the length of herniation of the cerebellar tonsils.

growth.

3. Statistical analyses

The patient groups were compared with normal controls, with patients and controls divided into 3-year age groups and 20 years or older than 20 years (Table 1). IBM SPSS statistics software (IBM Corp., Armonk, NY, USA) was used for statistical analyses. The means were compared between patients and normal controls using the Mann-Whitney U test. A p-value < 0.01 was used to determine significance. For multiple analyses, heavy palindromic tests were used. Abnormalities of VPCF, VAFM, and occipital

bone size were defined as values below 1.5 SD.

III. Results of volumetric and morphometric analyses

1. Volumetric and morphometric analyses of PCF and CCJ (Table 2)

The data regarding the development and growth of normal controls matched those of previous reports.^{21,22)}

VBPCF was not significantly different between the cases and controls in all age groups. Of the measured items, only VPCF, occipital bone size, and VAFM were significantly different between the cases and healthy controls. Using palindromic tests in multifactorial analyses, three

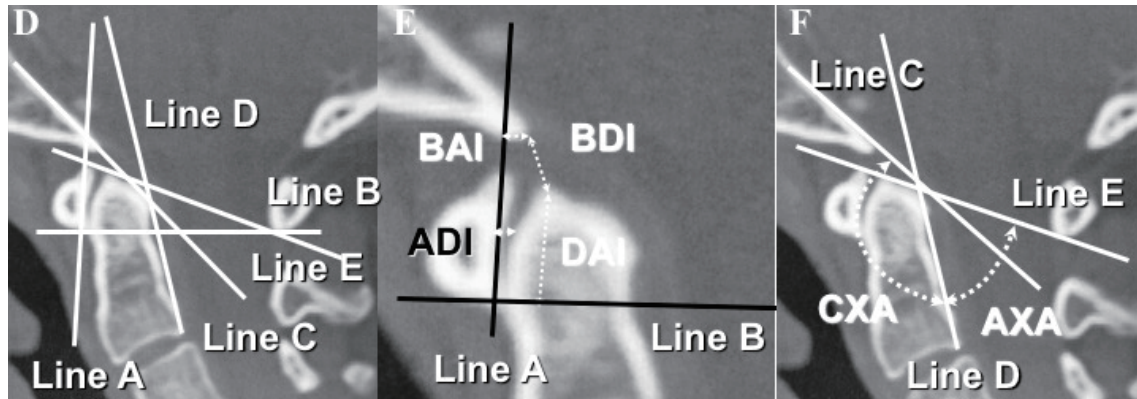


Fig. 2-2 Morphometric measurements of the posterior cranial fossa (PCF) and craniocervical junction (CCJ).

D: 2D-CT midline image of CCJ demonstrating the reference lines.

Line A indicates the plane of the posterior surface of the anterior arch of atlas. Line B indicates the line between the lowest point of the anterior arch of atlas and the lowest point of the posterior arch of atlas. Line C indicates the superior plane of the clivus. Line D indicates the plane of the posterior surface of dens. Line E indicates the plane of the top of the anterior arch of atlas and the lowest point of the posterior arch of atlas.

E and F: 2D-CT midline image demonstrating the morphometric measurements of ADI (interval between anterior arch and dens), BAI (interval between basion and Line A), BDI (interval between basion and top of dens), DAI (interval between top of dens and Line B), AXA (angle between axis [Line D] and atlas [Line E]), and CXA (angle between clivus [Line C] and axis [Line D]).

parameters (VPCF, VAFM, and occipital bone size) were used to classify the CM-I group into three independent groups: CM-I types A (160 cases), B (156 cases), and C (131 cases) (Table 1). CM-borderline (37 cases) indicated borderline small occipital bone size and small VAFM (-1.0 to -1.5 SD). In CM-I type B, C, and CM-borderline, the VBPCF/VPCF ratio in patients older than 4 years was significantly larger than that in the normal controls.

CM-I type A had normal VPCF, VAFM, and occipital bone size (Fig. 3A) in all age groups. CM-I type B had normal VPCF, small VAFM and occipital bone size, large volume of the PCF above the Twining's line (VPCF-ATW), and small volume of the PCF below the Twining's line (VPCF-BTW) (Fig. 3B) in all age groups. CM-I type C had small PCF, VAFM, and occipital bone size in all age groups (Fig. 3C). In CM-I types A, MH was decreased and 4VH was increased compared to controls in patients 8 or older than 8 years. In CM-I type C, MH was decreased and 4VH was increased compared to controls in all age groups. CM-borderline had normal VPCF and occipital bone size, but borderline small VAFM at ages 8 or older than 8 years (Fig. 3D).

2. Craniocervical traction test (Table 3)

The distance between the anterior arch of the atlas and dens (ADI) was used to evaluate the atlanto-axial horizontal dislocation. A change in ADI of 4 mm between flexion and extension is an accepted index of atlanto-axial horizontal dislocation.^{12,16-20} The vertical distance between the top part of dens and the lowest line of the axis (DAI) was used to evaluate the vertical basilar invagination. DAI > 15 mm from the top of dens above the McRae's line is an ac-

cepted index of basilar invagination.^{12,16-20} Furthermore, the morphometric analyses during craniocervical traction test revealed BDI, BAI, and CXA as reliable and reproducible measurements in patients with instability of occipito-atlanto-axial joints.

In the supine position, BDI, BAI, and CXA were normal. However, in the sitting position, the BDI decreased, BAI increased, and CXA decreased. During traction, these values returned to the normal range. In the follow-up evaluation of patients who underwent joint stabilization, normal values of BDI, BAI, and CXA were maintained. However, in patients without joint stabilization, these values were abnormal.

In 70 cases with instability, HDCT was present in 28 cases, bony anomalies (including basilar invagination) in 43 cases, and trauma in 18 cases. Among CM-I type A, CM-I type B, CM-I type C, and CM-borderline cases, 58 (36.3%), 3 (1.9%), 5 (3.8%), and 4 (10.8%) had instability, respectively. The proportion of CM-I type A cases with instability was higher than those in the other groups ($p < 0.01$).

Pathogenesis and Classification of CM-I (Fig. 3)

I. Mechanisms and pathogenesis of ptosis of the brainstem and cerebellum in CM-I type A (Fig. 3A, E, and F)

In patients with CM-I type A, VPCF, VAFM, occipital bone size, and VBPCF/VPCF were not significantly different compared to the control group. Therefore, the mechanism underlying ptosis of the brainstem and cerebellum was not the narrow space in the PCF, but rather was due to other mechanisms. In this study, CM-I type A cases

Table 1 Materials for morphometric and volumetric study

		4-7-year-old	8-11-year-old	12-15-year-old	16-19-year-old	20-49-year-old
Normal controls	150	20	24	23	25	58
Males and Females		8 and 12	10 and 14	11 and 12	11 and 14	24 and 34
Mean or median age (yrs.)		5.5 ± 1.41	9.4 ± 1.40	12.6 ± 1.37	17.7 ± 1.37	33.7 ± 10.2
CM-I type A	160	18	27	28	10	77
Males and Females		8 and 10	12 and 15	13 and 15	4 and 6	35 and 42
Mean or median age (yrs.)		5.4 ± 1.40	9.5 ± 1.44	12.5 ± 1.37	17.8 ± 1.35	33.2 ± 10.1
CM-I type B	156	17	24	25	10	80
Males and Females		7 and 10	11 and 13	12 and 13	4 and 6	35 and 45
Mean or median age (yrs.)		5.9 ± 1.38	10.1 ± 1.47	14.0 ± 1.34	17.7 ± 1.38	31.7 ± 10.8
CM-I type C	131	15	14	17	12	73
Males and Females		7 and 8	7 and 7	8 and 9	5 and 7	31 and 42
Mean or median age (yrs.)		5.8 ± 1.70	10.0 ± 1.70	13.7 ± 1.41	17.6 ± 1.37	38.7 ± 10.25
CM-borderline	37	3	4	5	5	20
Males and Females		1 and 2	2 and 2	2 and 3	2 and 3	8 and 12
Mean or median age (yrs.)		5.7 ± 1.41	9.4 ± 1.50	12.7 ± 1.35	17.8 ± 1.37	32.4 ± 10.4

Results are expressed as mean ± standard deviation.

Abbreviations: CM-I: Chiari malformation type I, CM-borderline: Chiari malformation borderline

demonstrated decreasing MH and increasing 4VH with the downward displacement of the brainstem and cerebellum (Fig. 3A). In CM-I type A, the downward displacement of the brainstem and cerebellum was observed in patients 8 or older than 8 years, which is in line with human development, suggesting that the mechanism underlying CM-I type A was not congenital, but rather acquired.

Milhorat, Bolognese, and other authors reported the phenomenon of functional cranial settling, in which the cranium (occipital bone) falls into the craniocervical junction.¹²⁾ This functional cranial settling may be the cause of ptosis of the brainstem and cerebellum (Fig. 3E and F). Goel et al. also reported that atlanto-axial instability might cause ptosis of the brainstem and cerebellum.¹⁶⁾ They reported evidence showing that atlanto-axial fixation resolved the instability and ptosis of the brainstem and cerebellum.^{12,16)} Among CM-I type A cases, almost 40% had CCJ instability, whereas among CM-borderline cases, 10% had CCJ instability. CM-I types B and C patients also had CCJ instability, but only in a few patients (1%-4%).

In addition, Milhorat and authors reported that tethering could cause ptosis of the brainstem and cerebellum due to traction. Traction at the tethered regions of the spinal cord and brainstem with the cerebellum could cause their downward displacement into the spinal canal (Fig. 3G).¹³⁾ They reported that sectioning of the filum terminale and/or lysis of adhesions in patients with CM-I type A and tethered cord syndrome may resolve the syrinx and allow the tonsil to rise.¹³⁾ The other mechanisms of ptosis of the brainstem and cerebellum include increased intracranial

pressure induced by intracranial hypertension and/or hydrocephalus, which results due to dissociation of pressure between the intracranial cavity and spinal canal cavity.^{3,23)}

The authors believe that the causes of CM-I type A are different from those of CM-I type B, CM-I type C, and CM-borderline, and these causes can be distinguished during surgical treatment. Therefore, CM-I type A should be treated differently from malformations, i.e., congenital etiology.

II. Mechanisms and pathogenesis of ptosis of the brainstem and cerebellum in CM-I types B and C, and CM-borderline (Fig. 3B-D)

Although the occipital bone size and VAFM were small in patients with CM-I type B, VPCF was normal because of compensation by the enlarged volume of the PCF above the Twining's line (VPCF-ATW) due to the steepness of the cerebellar tentorium. In individuals with CM-I type C, VPCF, VAFM, and occipital bone size were small. Increasing brain stem length (BSL) correlated with the elongation of the brainstem. Ptosis of the brainstem and cerebellum was caused by a small VAFM due to the underdevelopment of the occipital bone and large VBPCF/VPCF (Fig. 3B-D). This shallow space induced by the underdevelopment of occipital bone relative to the normal development of the brainstem and cerebellum results in overcrowding of the PCF, leading to sagging of the caudal brainstem and cerebellum into the spinal canal, similar to ptosis and elongation of the brainstem.

Occipital bone size and VAFM were small in patients

Table 2-1 Results of volumetric analyses

	4-7-year-old	8-11-year-old	12-15-year-old	16-19-year-old	20-49-year-old
Volumetric analysis: Normal controls (150 cases)	20	24	23	25	58
VPCF (mL)	178.2 ± 9.48	181.7 ± 9.36	185.8 ± 9.54	188.7 ± 8.42	189.4 ± 8.77
VPCF-ATL (mL)	38.1 ± 4.74	40.5 ± 5.28	42.8 ± 5.12	43.8 ± 5.12	44.2 ± 5.10
VPCF-BTL (mL)	140.7 ± 4.88	141.0 ± 4.17	142.6 ± 4.45	145.0 ± 4.17	147.6 ± 4.38
VAFM (mL)	21.7 ± 3.12	22.5 ± 3.24	23.0 ± 3.25	24.8 ± 3.24	25.3 ± 3.22
VBPCF (mL)	144.5 ± 3.45	147.8 ± 3.21	148.8 ± 3.11	149.8 ± 3.12	150.1 ± 3.13
Volumetric analysis: CM-I type A (160 cases)	18	27	28	10	77
VPCF (mL)	179.0 ± 9.40	181.7 ± 9.33	185.8 ± 9.54	188.5 ± 8.40	189.8 ± 8.75
VPCF-ATL (mL)	38.1 ± 4.73	40.2 ± 5.25	43.8 ± 5.13	44.8 ± 5.12	44.2 ± 5.12
VPCF-BTL (mL)	140.8 ± 4.82	141.5 ± 4.13	142.0 ± 4.42	144.0 ± 4.17	145.6 ± 4.45
VAFM (mL)	21.7 ± 3.14	22.7 ± 3.23	23.02 ± 3.24	25.2 ± 3.24	25.4 ± 3.24
VBPCF (mL)	145.5 ± 3.45	148.7 ± 3.22	148.5 ± 3.18	151.0 ± 3.15	151.2 ± 3.14
Volumetric analysis: CM-I type B (156 cases)	17	24	25	10	80
VPCF (mL)	154.3 ± 8.87	162.3 ± 9.16	164.1 ± 8.64	188.7 ± 8.42	189.4 ± 8.77
VPCF-ATL (mL)	42.2 ± 4.35†	47.7 ± 4.84†	54.1 ± 4.84†	64.8 ± 5.12†	65.2 ± 5.10†
VPCF-BTL (mL)	112.1 ± 5.10	115.4 ± 5.05	117.0 ± 5.73	123.8 ± 5.34	124.0 ± 5.44
VAFM (mL)	13.7 ± 3.12*	17.5 ± 3.28*	18.0 ± 3.41*	19.8 ± 3.24*	20.3 ± 3.43*
VBPCF (mL)	141.5 ± 4.34	146.5 ± 4.48	147.6 ± 4.42	150.0 ± 3.44	150.1 ± 3.46
Volumetric analysis: CM-I type C (131 cases)	15	14	17	12	73
VPCF (mL)	160.7 ± 8.27*	172.4 ± 8.18*	173.4 ± 8.63*	181.7 ± 8.42*	182.4 ± 8.77*
VPCF-ATL (mL)	33.1 ± 4.34*	34.7 ± 4.96*	35.2 ± 5.35*	37.8 ± 5.10*	38.5 ± 5.14*
VPCF-BTL (mL)	127.6 ± 7.10*	138.5 ± 7.40*	139.8 ± 7.20*	142.8 ± 7.31*	144.0 ± 7.31*
VAFM (mL)	12.7 ± 3.02*	16.5 ± 3.22*	17.04 ± 3.25*	17.8 ± 3.45*	18.8 ± 3.34*
VBPCF (mL)	145.7 ± 4.61	148.7 ± 4.67	149.8 ± 4.07	150.8 ± 3.22	152.1 ± 3.23
Volumetric analysis: CM-borderline (37 cases)	3	4	5	5	20
VPCF (mL)	177.2, 178.4, 178.5	181.2 ± 8.44	185.0 ± 9.51	187.6 ± 8.54	189.5 ± 8.54
VPCF-ATL (mL)	35.6, 38.2, 38.5	40.2 ± 5.38	41.9 ± 5.23	43.0 ± 5.04	44.8 ± 5.32
VPCF-BTL (mL)	138.2, 140.5, 142.4	141.7 ± 4.27	142.8 ± 4.52	143.8 ± 4.51	145.0 ± 4.47
VAFM (mL)	16.1, 21.5, 21.7	19.4 ± 3.25*	20.2 ± 3.47*	20.8 ± 3.23*	21.2 ± 3.53*
VBPCF (mL)	142.2, 144.5, 146.2	146.9 ± 3.43	147.8 ± 3.25	150.1 ± 3.42	150.8 ± 3.43

Results are expressed as value ± standard deviation.

*: significantly smaller or shorter than those of normal controls ($p < 0.01$).

†: significantly longer or larger than those of normal controls ($p < 0.01$).

Abbreviations: VPCF: volume of the posterior cranial fossa, VPCFV-ATL: volume of the posterior cranial fossa above Twining's line, VPCF-BTL: volume of the posterior cranial fossa below Twining's line, VAFM: volume of the area of the foramen magnum, VBPCF: the volume of the brain in the posterior cranial fossa

with CM-borderline, so we hypothesized that the mechanism underlying ptosis of the brainstem and cerebellum was also underdevelopment of the occipital bone and shallowness of the surrounding area of the foramen magnum, which was a focal condition. In this type, the foramen magnum and major cisterns demonstrated tightness and compression of the brainstem and cerebellar tonsils and vermis, which caused neurological symptoms and interfered with the CSF flow.

In patients with CM-I type C, the brainstem was elon-

gated and both the brainstem and cerebellum were displaced downward (Fig. 3C). In CM-I type C, the decreasing MH and increasing 4VH demonstrated downward displacement of the brainstem and cerebellum, which worsened the situation. In CM-I type C, the downward displacement of the brainstem and cerebellum was confirmed since the age of early infancy, suggesting that it is caused by congenital factors. Taylor et al. identified two distinct populations of Chiari malformation based on the presence or absence of PCF "crowdedness".²⁴⁾

Table 2-2 Results of morphometric measurements of the occipital bone

	4-7-year-old	8-11-year-old	12-15-year-old	16-19-year-old	20-49-year-old
Occipital bone size: Normal controls (150 cases)	20	24	23	25	58
Clivus: axial length (mm)	40.2 ± 3.87	42.5 ± 4.12	45.7 ± 3.96	46.8 ± 3.67	47.5 ± 3.55
Supraocciput axial length (mm)	41.5 ± 3.35	44.7 ± 4.28	46.7 ± 3.64	47.2 ± 3.53	46.8 ± 3.64
Condyle axial height at the right (mm)	20.2 ± 2.16	21.4 ± 2.25	22.8 ± 2.34	23.7 ± 3.65	24.0 ± 3.24
axial height at the left (mm)	20.4 ± 2.21	21.3 ± 2.27	22.7 ± 2.31	23.5 ± 3.54	23.9 ± 3.32
Occipital bone size: CM-I type A (160 cases)	18	27	28	10	77
Clivus: axial length (mm)	41.2 ± 3.87	42.3 ± 4.12	45.5 ± 3.96	47.3 ± 3.65	47.4 ± 3.54
Supraocciput axial length (mm)	41.5 ± 3.27	43.9 ± 4.21	45.7 ± 3.65	47.4 ± 3.53	47.8 ± 3.62
Condyle axial height at the right (mm)	20.2 ± 2.16	21.4 ± 2.25	22.8 ± 2.34	23.7 ± 3.65	24.0 ± 3.24
axial height at the left (mm)	20.5 ± 2.22	21.3 ± 2.27	22.7 ± 2.31	23.5 ± 3.54	23.9 ± 3.32
Occipital bone size: CM-I type B (156 cases)	17	24	25	10	80
Clivus: axial length (mm)	34.7 ± 3.26*	36.1 ± 3.42*	37.1 ± 3.11*	39.8 ± 3.13*	40.5 ± 3.50*
Supraocciput axial length (mm)	33.2 ± 3.15*	37.8 ± 3.98*	38.4 ± 3.12*	40.2 ± 3.48*	86.8 ± 3.64*
Condyle axial height at the right (mm)	14.7 ± 3.15*	15.8 ± 3.24*	17.6 ± 2.52*	18.7 ± 3.54*	20.0 ± 3.42*
axial height at the left (mm)	14.8 ± 3.27*	16.0 ± 3.31*	7.9 ± 2.78*	18.4 ± 3.50*	20.9 ± 3.25*
Occipital bone size: CM-I type C (131 cases)	15	14	17	12	73
Clivus: axial length (mm)	41.8 ± 3.27*	43.1 ± 3.72*	44.9 ± 4.17*	45.5 ± 3.44*	45.6 ± 3.24*
Supraocciput axial length (mm)	41.7 ± 3.54*	41.8 ± 3.76*	46.8 ± 3.94*	45.2 ± 3.33*	46.3 ± 3.43*
Condyle axial height at the right (mm)	20.8 ± 3.73*	20.8 ± 3.14*	22.4 ± 2.94*	23.3 ± 3.65*	23.5 ± 3.22*
axial height at the left (mm)	20.2 ± 3.24*	21.4 ± 3.07*	22.8 ± 2.34*	23.4 ± 3.54*	23.9 ± 3.31*
Occipital bone size: CM-borderline (37 cases)	3	4	5	5	20
Clivus: axial length (mm)	38.5, 39.4, 40.2	42.2 ± 4.23	45.1 ± 3.78	46.4 ± 3.54	47.4 ± 3.36
Supraocciput axial length (mm)	40.2, 41.5, 42.2	44.8 ± 4.83	47.2 ± 3.55	47.0 ± 3.42	47.8 ± 3.77
Condyle axial height at the right (mm)	19.5, 20.4, 21.3	21.8 ± 2.72	22.7 ± 2.33	23.8 ± 3.67	24.0 ± 3.24
axial height at the left (mm)	20.4 ± 2.21	21.3 ± 2.27	22.7 ± 2.31	23.5 ± 3.54	23.9 ± 3.32

Results are expressed as value ± standard deviation.

*: significantly smaller or shorter than those of normal controls ($p < 0.01$).

Abbreviations: CM-I: Chiari malformation type I, CM-borderline: Chiari malformation borderline

III. Developmental and embryological aspects of the pathogenesis of CM-I

The fundamental pathological mechanism underlying CM-I types B and C, and CM-borderline is underdevelopment of the occipital bone. During development, the occipital bone is formed from the enchondral bone, which originates from occipital somites. Therefore, the pathogenesis of CM-I types B and C may be related to insufficiency of the para-axial mesoderm as the source of occipital somite.^{1,3} Speer et al. proved the existence of a mutation in an unidentified gene that influenced segmentation of the mesoderm and neural tube.^{9,10} Milhorat et al. reported that there were some families with CM-I with an underlying genetic basis that was inherited in an autosomal dominant pattern.²

Conversely, CM-I type C is characterized by severe disproportion between the occipital bone and brain. However, during surgery, although the running up of lower cranial

nerves and C1 and 2 roots was observed, the anatomical relationship between the original location of the nerves and foramina was normal. This evidence suggests that the segmentation and migration of neural crest cells was normal. The authors suggest that the displacement of the brainstem and cerebellum indicates misalignment of segmentation between occipital somite and hindbrain at the early embryonic stage.^{25,26} In addition, in the late fetal period, when the brainstem and cerebellum rapidly develop and grow, the additional force as traction and/or squeezing may cause elongation and downward displacement of the brainstem and cerebellum.²⁷

Decision of Surgical Intervention and Its Procedures

Chiari malformation is managed using appropriate surgical methods that can treat ptosis of the brainstem and

Table 2-3 Results of morphometric measurements of the neural structures in the posterior cranial fossa

	4-7- year-old	8-11-year-old	12-15-year-old	16-19-year-old	20-49-year-old
Neural structures: Normal controls (150 cases)	20	24	23	25	58
Brain stem length (BSL) (mm)	44.7 ± 3.55	47.5 ± 2.43	48.8 ± 2.74	50.1 ± 2.45	51.2 ± 2.34
Medullary height (MH) (mm)	12.8 ± 3.35	15.2 ± 4.42	17.5 ± 3.38	18.1 ± 4.55	18.4 ± 4.25
4th Ventricle height (4VH) (mm)	2.37 ± 3.21	3.24 ± 2.76	3.64 ± 2.97	4.11 ± 3.58	4.18 ± 3.12
Neural structures: CM-I type A (160 cases)	18	27	28	10	77
Brainstem length (BSL) (mm)	45.7 ± 3.58	47.7 ± 2.42	48.7 ± 2.73	50.0 ± 2.43	51.2 ± 2.32
Medullary height (MH) (mm)	13.0 ± 3.28	12.4 ± 4.40*	11.8 ± 3.41*	10.1 ± 4.55*	10.4 ± 4.27*
4th Ventricle height (4VH) (mm)	2.37 ± 3.22	6.25 ± 2.78†	6.65 ± 2.96†	8.12 ± 3.60†	8.17 ± 3.14†
Neural structures: CM-I type B (156 cases)	17	24	25	10	80
Brain stem length (BSL) (mm)	45.5 ± 2.21	50.6 ± 2.02	51.8 ± 2.27	50.2 ± 2.47	51.3 ± 2.44
Medullary height (MH) (mm)	14.1 ± 2.24	15.8 ± 2.69	16.0 ± 2.95	18.0 ± 4.52	18.4 ± 4.27
4th Ventricle height (4VH) (mm)	2.40 ± 2.18	3.17 ± 3.57	4.05 ± 3.24	4.12 ± 3.57	4.15 ± 3.15
Neural structures: CM-I type C (131 cases)	15	14	17	12	73
Brain stem length (BSL) (mm)	47.7 ± 1.73†	47.3 ± 2.53	48.5 ± 2.56	50.4 ± 2.55	51.0 ± 2.65
Medullary height (MH) (mm)	6.9 ± 2.8*	12.4 ± 4.38*	27.0 ± 3.42*	12.7 ± 4.65*	12.8 ± 4.43*
4th Ventricle height (4VH) (mm)	4.87 ± 2.1†	5.44 ± 2.82†	6.63 ± 2.95†	7.12 ± 3.60†	7.20 ± 3.52†
Neural structures: CM-borderline (37 cases)	3	4	5	5	20
Brain stem length (BSL) (mm)	42.3, 44.2, 44.9	47.3 ± 2.53	48.5 ± 2.56	50.4 ± 2.55	51.0 ± 2.65
Medullary height (MH) (mm)	10.4, 12.8, 13.4	15.4 ± 4.38	17.0 ± 3.42	18.4 ± 4.65	18.8 ± 4.43
4th Ventricle height (4VH) (mm)	1.23, 2.47, 2.55	3.44 ± 2.82	3.63 ± 2.95	4.12 ± 3.60	4.20 ± 3.52

Results are expressed as value ± standard deviation.

*: significantly smaller or shorter than those of normal controls ($p < 0.01$).

†: significantly longer or larger than those of normal controls ($p < 0.01$).

Abbreviations: CM-I: Chiari malformation type I, CM-borderline: Chiari malformation borderline

cerebellum.^{28,29)} Therefore, we selected foramen magnum decompression (FMD) for CM-I type B and CM-borderline cases, because VAFM and occipital bone size were small in these patients. FMD consists of craniectomy of the surrounding area of the foramen magnum (2-3-cm square), decompression of the brainstem and cerebellum, and creation of major cisterns and flow out of CSF from the foramina of Magendie and Luschka.^{30,31)} The authors suggest that FMD is adequate for CM-I type B and CM-borderline with small VAFM but normal VPCF.

Conversely, in CM-I type C, it is necessary to expand the entire PCF and remodel the relationship between the brain and occipital bone. According to Sakamoto and the authors,^{31,32)} expansive suboccipital cranioplasty (ESCP) involves extensive decompression to expand the surrounding area of the foramen magnum and the entire PCF (along the transverse sinus and sigmoid sinus), C1 laminectomy, dural plasty, and osteoplasty to maintain the PCF expansion. ESCP can normalize the VPCF and major cisterns, which is adequate for the decompression of the brainstem and cerebellum, and to remodel the appropriate positional relationship between the brainstem, cerebellum, and occipital bone by expanding the entire PCF, including C1. We

selected ESCP for CM-I type C because FMD was not adequate under the setting of small VAFM, small VPCF, and small occipital bone size.

In CM-I type A, other surgical methods that can treat ptosis of the brainstem and cerebellum must be selected. Craniocervical posterolateral fixation (CCF) should be selected for cases with craniocervical instability causing functional cranial settling.^{12,16)} It is important to identify the occipito-atlanto-axial joints with instability, and determine the appropriate method of screw insertion. The most important anchor for screw insertion is C2, and a pedicle screw is the ideal choice for C2.

Surgical Intervention for CM-I, CM-borderline, and Instability

I. Materials and methods

1. Surgical indications and patient population

Surgery was performed in cases of myelopathy, upper cervical cord symptoms, brainstem symptoms, and Japanese Orthopaedic Association (JOA) score < 14 .³³⁾

In total, 484 patients underwent surgical treatment: 302 underwent FMD, 104 underwent ESCP, and 70 underwent

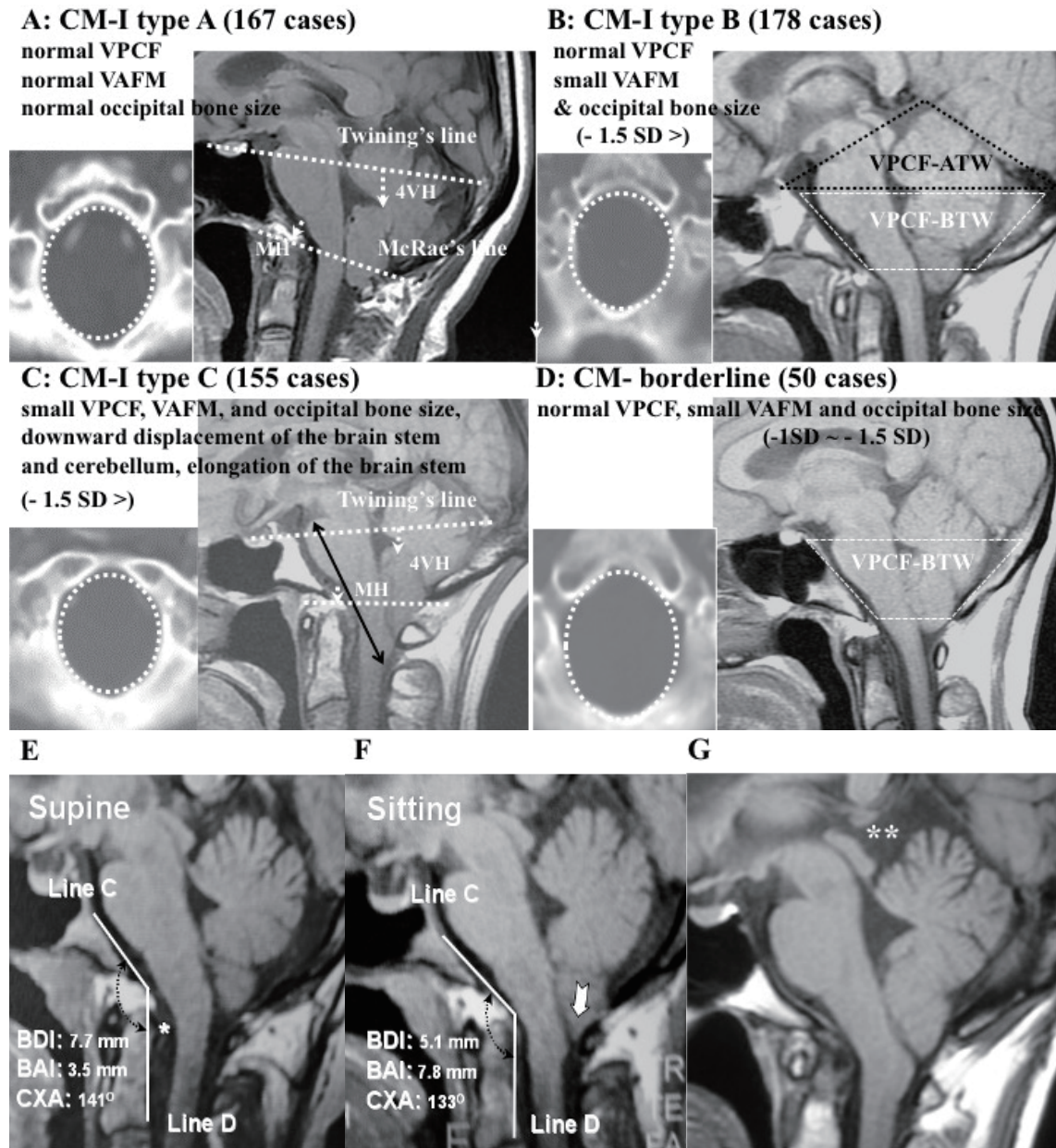


Fig. 3 Illustrative cases of CM-I types A, B, and C, and CM-borderline.

Pictures were reprinted and modified from [16].

Left panel: 2D-CT axial image at the level of the foramen magnum; right panel: magnetic resonance (MR) sagittal midline image.

A: CM-I type A; B: CM-I type B; C: CM-I type C; D: CM-borderline;

E and F: MR midsagittal images demonstrating the character of CM-I with HDCT. The VPCF, VAFM, and occipital bone size were normal in size.

E: MR midsagittal image in supine position showing normal BDI (7.7 mm), normal BAI (3.5 mm), normal CXA (141°), large retro-odontoid pannus (asterisk), and low-lying cerebellar tonsils.

F: On the assumption of the upright position, there was cranial settling (2.5 mm decrease in BDI), posterior gliding of occipital condyle (4.3 mm increase in BAI), anterior flexion of the occipito-atlantal joint (8° decrease in CXA), and increased cerebellar ptosis with downward displacement of cerebellar tonsils to C1 (white arrow). Note the greatly increased impaction of the foramen magnum anteriorly and posteriorly.

Bilateral black dotted arrow = CXA, asterisk = retro-odontoid pannus, white arrow = tonsillar herniation.

G: MR midsagittal image demonstrating the character of CM-I type A with TCD. VPCF, VAFM, and occipital bone size were normal in size. MR image showing elongation and downward displacement of the brainstem and cerebellum, and a large supracerebellar cistern (double asterisk).

Abbreviations: HDCT = hereditary disorders of connective tissue

Table 3 Results of morphometric measurements of craniocervical junction in the craniocervical traction test

	Normal Controls 30 cases (12-year-old≤)	Craniocervical test		During operation in positioning	Follow up CSJ cases	Follow up ICSJ cases
		Nontraction	Traction			
ADI (mm)						
Flexion position in sitting	3.4 ± 0.47	7.4 ± 1.24‡	3.3 ± 0.55	N.A.	3.4 ± 0.53	7.4 ± 1.24‡
Neutral position in sitting	2.8 ± 0.54	3.1 ± 0.63	3.0 ± 0.51	3.2 ± 0.45	3.0 ± 0.48	3.1 ± 0.63
Extension position in sitting	2.0 ± 0.48	2.3 ± 0.58	2.7 ± 0.47	N.A.	3.2 ± 0.52	2.3 ± 0.58
Supine position	2.8 ± 0.57	2.4 ± 0.34	2.5 ± 0.74	in positioning	2.2 ± 0.64	2.5 ± 0.52
Sitting position	2.4 ± 0.58	2.1 ± 0.42	1.94 ± 0.44	2.2 ± 0.781	2.4 ± 0.68	2.3 ± 0.64
BAI (mm)						
Supine position	1.8 ± 1.21	2.0 ± 1.25	2.2 ± 1.52	in positioning	2.2 ± 1.30	2.5 ± 1.48
Sitting position	2.1 ± 1.88	5.1 ± 1.22‡	1.85 ± 0.71	2.0 ± 1.21	2.3 ± 1.38	5.3 ± 1.57‡
BDI (mm)						
Supine position	7.4 ± 1.58	8.7 ± 1.70	8.8 ± 2.23	in positioning	8.3 ± 1.82	7.6 ± 2.01
Sitting position	7.2 ± 1.59	3.9 ± 1.81†	8.4 ± 2.20	8.7 ± 2.70	8.2 ± 1.84	3.8 ± 1.92†
AXA (°)						
Supine position	37.6 ± 6.55	35.2 ± 5.44	4.72 ± 6.23	in positioning	34.5 ± 6.04	35.3 ± 5.43
Sitting position	37.4 ± 6.84	36.5 ± 5.96	35.8 ± 5.88	36.7 ± 6.40	35.4 ± 5.44	34.4 ± 5.41
CXA (°)						
Supine position	147.6 ± 6.61	145.2 ± 5.27	146.5 ± 5.68	in positioning	144.8 ± 5.49	145.8 ± 5.58
Sitting position	147.8 ± 6.00	136.8 ± 6.47†	145.4 ± 5.88	146.8 ± 6.45	145.2 ± 5.58	134.2 ± 5.58†

Results are expressed as mean ± one standard deviation.

†: significantly smaller than those of normal controls ($p < 0.01$).

‡: significantly larger than those of normal controls ($p < 0.01$).

Abbreviations: CSJ: complete stabilization of joints, ICSJ: incomplete stabilization of joints, ADI: the distance between the atlas and dens, BAI: the distance between basion and anterior arch of the atlas, BDI: the distance between basion and top of dens, AXA: the angle between the atlas and axis, CXA: the angle between clivus and axial, N.A.: not applicable

CCF. 10 patients underwent ventricle peritoneal shunt and 10 underwent section filum terminale and/or lysis of the adhesion of the spinal cord.

The patient group for surgical interventions was the same as that for the volumetric and morphometric study. The patients were treated between April 2002 and March 2020 at the institute or hospitals as described above.

2. Operative procedures for CM-I types B and C, and CM-borderline

After decompression and opening the dura mater, normalized CSF flow was confirmed using color Doppler ultrasonography (CDU).³⁴⁾ If normalized CSF flow was not observed, the arachnoid membrane was opened. In such cases, the arachnoid veil or regional adhesions may interfere with CSF outflow from the foramina of Magendie and Luschka. Therefore, lysis of adhesions was performed.

In children younger than 12 years, the cranium and brain are under development, so the possibility of disproportion between the cranium and brain changes over time. For patients younger than 12 years, FMD was performed

first.

3. Operative procedures for CM-I type A and instability

CCF was performed for CCJ instability.^{35,36)} If the patient had instability at the occipito-atlanto-axial joints, occipito-cervical posterolateral fixation (OCF) should be performed. For patients with instability at the atlanto-axial joints alone, C1/2 posterolateral fixation (C1/2 FIX) should be performed. In cases where a pedicle screw could be inserted for C2, fixation of C2 with screws was adequate. In cases where screw insertion was not possible, it was necessary to fix C2 to C3 or C4.

CCF was performed in a total of 70 cases, of which C1/2 FIX was performed in 36 cases and OCF in 34 cases. For cases (7 cases) with CCJ instability associated with CM-I types B and C, and CM-borderline, staged CCF combined with ESCP or FMD was performed.³⁷⁾

In children younger than 12 years, the relationships between anatomical structures are under development, so there is a possibility of overestimating instability. In children, the loss of function of occipito-atlanto-axial joints in-

duces significant handicap. Therefore, CCF was not performed in children younger than 12 years.

4. Neurological and neuroradiological examinations, follow-up, and statistical analyses

Postoperatively, the neurological symptoms and signs, JOA score, recovery rate of JOA score (JOA score RR) ($[(\text{postoperative points} - \text{preoperative points}) / (\text{full points} - \text{preoperative point})] \times 100\%$),³³⁾ and neuroradiological findings (cervical spine dynamic X-ray, 2D-CT, and MRI of the cervical spine) were examined every 3 months. Persistent syringomyelia was defined by confirmation of syringomyelia larger than 2 mm in diameter.

Surgical outcome was assessed using χ^2 and Fisher's tests. A p-value < 0.01 was used to determine significance.

II. Results of surgical intervention

The follow-up duration was 24-216 months (mean: 88.5 months). The results were based on the most recent data. In total, 58 patients were lost to follow-up after more than 3 years of operation, in whom the results of the final examination were estimated.

1. Results of JOA score and its RR after FMD and ESCP (Table 3)

Among adults and adolescents aged 12 years and older, the improvement rate for neurological symptoms and signs in FMD was 87.8%. The JOA score RR in FMD was 58.7%, and 92.2% of cases showed improvement or stabilization of the neurological symptoms. In 14 cases (7.8%), the neurological symptoms deteriorated during follow-up. In 10 out of 127 cases with syringomyelia (7.9%), the symptoms persisted. The improvement rate for neurological symptoms and signs in ESCP was 88.4%. The JOA score RR in ESCP was 60.2%, and 98.0% of cases had an improvement or stabilization of neurological symptoms. In two cases (2.0%), the neurological symptoms deteriorated during follow-up. In 1 out of 38 cases with syringomyelia (2.6%), the symptoms persisted. There was no significant difference between the FMD and ESCP groups in terms of improvement or stabilization of neurological symptoms and JOA score RR. Persistent syringomyelia and deterioration of neurological symptoms and/or signs were significantly more common in patients who underwent FMD compared to ESCP ($p > 0.01$).

In children younger than 12 years, the improvement rate for neurological symptoms and/or signs was significantly lower in CM-I types A (68.9%) and C (69.0%) than in CM-I type B (80.5%) and CM-borderline (85.7%) ($p > 0.01$). The JOA score RR was significantly lower in CM-I type C (48.6%) than in CM-I type A (57.2%), CM-I type B (58.2%), and CM-borderline (54.3%) ($p > 0.01$). Persistent syringomyelia and deterioration in neurological symptoms and/or signs were significantly more common in patients with CM-I types A (33.3% and 31.1%, respectively) and C (50.0%

and 34.5%, respectively) than in CM-I type B (3.3% and 4.2%, respectively) and CM-borderline (0% and 0%, respectively) ($p > 0.01$).

2. Results of JOA score and its RR after CCF (Table 4)

The JOA score RR for the 70 cases who underwent CCF was 69.7%. In total, 46 cases (67.1%) had complete bony fusion, 59 (84.3%) had stabilized joints, and 11 (15.7%) had incomplete stabilization. Syringomyelia resolved in all 21 cases.

The preoperative JOA score was significantly lower in OCF than in C1/2 FIX. In 36 cases who underwent C1/2 FIX, the JOA score RR was 78.7%. In total, 26 cases (72.2%) had complete bony fusion, 32 (88.9%) had stabilized joints, and 4 (11.1%) had incomplete stabilization. The JOA score RR in the 34 cases who underwent OCF was 63.5%. In total, 21 cases (61.8%) had complete bony fusion, 27 (79.4%) had stabilized joints, and 7 (20.6%) had incomplete stabilization. In cases who underwent C1/2 FIX, the JOA score RR, stabilization rate, and rate of bony fusion of joints were higher than those in cases who underwent OCF.

3. Complications and side effects

In the FMD and ESCP groups, there was no mortality or permanent morbidity. Total transient morbidity occurred in 10 cases (2.5%). Complications were observed in six cases (2.0%) with FMD and four cases (3.9%) with ESCP. After FMD, two cases (0.7%) had wound infections, one (0.3%) had arachnoid adhesions, and one (0.3%) had CSF leakage. After ESCP, two cases (2.0%) had wound infection, one (1.0%) had cerebellar slugging without neurological symptoms, and one (1.0%) had CSF leakage. Repetitive and persistent neck pain continued in three cases (2.9%) with ESCP. There were significantly more frequent complications and side effects after ESCP than those after FMD.

In both C1/2 FIX and OCF, there was no mortality or permanent morbidity. Transient morbidity occurred in two cases (2.9%). The complications included transient swallowing disturbance in one case (1.4%) after OCF and injury to the vertebral artery without neurological symptoms in one case (1.4%) after C1/2 FIX. After OCF, repetitive and persistent neck pain continued in three cases (8.8%) and functional loss of visual fields occurred in two cases (5.9%). There were significantly more frequent complications and side effects after OCF than C1/2 FIX.

Discussion about Outcomes of Surgical Interventions

I. Outcomes of surgical intervention after FMD and ESCP (Table 4)

Among children aged younger than 12 years, the improvement rate of neurological symptoms and/or signs was significantly lower in CM-I type A than in CM-I type B and CM-borderline, and the rate of persistent syringomye-

Table 4 Japanese Orthopaedic Association score and its recovery rate after foramen magnum decompression and expansive suboccipital cranioplasty

	Improved neurological symptoms/signs	JOA score RR (%) (mean with ± 1 SD)	Re-syringomyelia	Stabilized neurological symptoms/signs	Deteriorated neurological symptoms/signs	Transient morbidities
Total number: 404 cases	339/404 (83.9%)	58.5 \pm 10.4	21/221 (9.5%)	24/404 (5.9%)	42/406 (10.4%)	10/404 (2.5%)
12 years or older (≥ 12 years)						
FMD: 180 cases (for CM-I types A, B and CM-borderline)	158/180 (87.8%)	58.7 \pm 10.2	10/127 (7.9%) *	8/180 (4.4%)	14/180 (7.8%) *	3/180 (1.7%)
ESCP102 cases (for CM-I type C)	90/102 (88.2%)	60.2 \pm 10.1	1/38 (2.6%)	10/102 (9.8%)	2/102 (2.0%) *	4/104 (3.9%) *
Younger than 12 years (< 12)						
FMD for all types: 122 cases						
CM-I type A: 45 cases	31/45 (68.9%) **	57.2 \pm 9.1	4/12 (33.3%) *	0/45 (0%)	14/45 (31.1%) *	1/45 (2.2%)
CM-I type B: 41 cases	34/41 (80.5%)	58.2 \pm 10.1	1/30 (3.3%)	5/41 (12.2%)	2/41 (4.2%)	1/41 (2.4%)
CM-I type C: 29 cases	20/29 (69.0%) **	48.6 \pm 10.2**	5/10 (50.0%) *	0/29 (0%)	10/29 (34.5%) *	1/29 (3.4%)
CM-borderline: 7 cases	6/7 (85.7%)	54.3 \pm 10.4	0/4 (0%)	1/7 (14.2%)	0/7 (0%)	0/7 (0%)

*: significantly higher or more than the other groups ($p < 0.01$).

**: significantly lower or less than the other groups ($p < 0.01$).

Abbreviations: JOA score: Japanese Orthopedic Association score, JOA score RR: recovery rate of the Japanese Orthopedic Association score, Re-syringomyelia: syringomyelia remaining, SD: standard deviation, FMD: foramen magnum decompression, CM-I: Chiari malformation type I, CM-borderline: the cases which have neurological brain stem and/or myelopathy, but tonsillar herniation less than 5 mm, ESCP: expansive suboccipital cranioplasty

lia and deterioration of neurological symptoms and/or signs were significantly more common in CM-I type A than in CM-I type B and CM-borderline. These data suggest that in CM-I type A, FMD is not the most appropriate treatment of the mechanism of ptosis of the brainstem and cerebellum. Therefore, other operative procedures should be considered.

Among patients younger than 12 years, the improvement rate for neurological symptoms and/or signs and the JOA score RR were significantly lower in CM-I type C than in CM-I type B and CM-borderline. In addition, the rate of persistent syringomyelia and deterioration of neurological symptoms and/or signs were significantly more common in CM-I type C than in CM-I type B and CM-borderline. These data suggest that in CM-I type C, FMD was unable to resolve the mechanism of ptosis of the brainstem and cerebellum and was not adequate to decompress the brainstem and cerebellum or normalize the CSF flow at the foramen magnum. Therefore, additional decompression should be considered. In children aged younger than 12 years, CM-I type C should be treated with ESCP or two-staged surgery, with initial FMD followed by observation, and in case of worsening neurological symptoms and/or signs or persistent syringomyelia, ESCP should be performed.

Among patients aged 12 years and older, both ESCP and FMD are associated with good surgical outcomes. The outcomes reported in the present study were better than those reported previously in cases who underwent FMD

only. In addition, morbidity and complications occurred less frequently in the present study than in previous reports.³⁸⁻⁴⁰ This suggests that the selection of surgical procedures (i.e., ESCP or FMD) according to the morphometric analyses was appropriate.

We believe that it is essential to confirm the normalization of CSF flow at the foramen magnum during the operation. If CSF flow is not normalized with dural opening, more extensive decompression, opening of the arachnoid membrane, lysis of foramina of Magendie and Luschka, and/or shrinkage of tonsils should be considered. Milhorat et al. proposed a tailored operation for patients so that the operative procedures should be selected based on the CSF flow dynamics assessed using CDU.²⁷ We decided regarding the need for extensive craniotomy and dural plasty, as well as shrinkage of tonsils, based on the CSF flow dynamics assessed using CDU during the operation. We suggest that the CSF flow can be normalized by initial decompression by enlargement of the craniotomy, followed by dural opening and plasty, and finally by shrinkage of the cerebellar tonsils.

II. Outcome of CCF for instability of occipito-atlanto-axial joints (Table 5)

For CCF, both C1/2 FIX and OCF achieved high rates of improvement of neurological symptoms and stabilization and/or bony fusion of joints.^{35,36,41} Our results were superior than those of previous reports of CCF,^{35,36,41} which suggested that surgical treatment of CCF was effective for cra-

Table 5 Japanese Orthopaedic Association score and its recovery rate after craniocervical fixation

Operative procedures	Improved neurological symptoms/signs	Preop. JOA score (mean ± 1 SD)	Postop. JOA score (mean ± 1 SD)	JOA score RR (%)	Bony fusion of joints	Stabilization of joints
CCF: 70 cases	65/70 (92.9%)	4-15 (9.7 ± 2.48)	10-17 (15.5 ± 2.51)	69.7%	47/70 (67.1%)	59/70 (84.3%)
C1/2 FIX 36 cases	34/36 (94.4%)	4-12 (9.0 ± 2.55) *	14-17 (15.4 ± 2.58)	78.7%*	26/36 (72.2%) *	32/36 (88.9%) *
OCF 34 cases	32/34 (94.1%)	3-12 (6.4 ± 2.43)**	10-17 (15.7 ± 2.48)	63.5%**	21/34 (61.8%) **	27/34 (79.4%) **

*: significantly higher than OCF ($p < 0.01$).

** : significantly lower than C1/2 FIX ($p < 0.01$).

Abbreviations: JOA score: Japanese Orthopedic Association score, JOA score RR: recovery rate of Japanese Orthopedic Association score, SD: standard deviation, CCF: craniocervical fixation, C1/2 FIX: atlantoaxial posterior lateral fixation, OCF: occipitocervical fixation

nial settling due to craniocervical instability. OCF leads to a greater loss of function and more frequent complications and side effects due to the fixing of occipito-atlanto-axial joints compared to C1/2 FIX. Therefore, patients for fixation, including that of the occipital bone, should be carefully selected. Craniocervical traction test was useful to detect instability at the occipito-atlantal joints and risk of loss of function by fixation.

Using morphometric analyses during craniocervical traction test, we detected the instability, hypermobility, and dislocation of occipito-atlanto-axial joints. The morphometric analyses also helped to select the treatment method for joint fixation, determine the symptoms of instability, and confirm whether the instability was reducible. It is necessary to recognize the advantages and disadvantages of joint fixation, including possible loss of joint function. It is necessary to consider the effects of OCF and C1/2 FIX on swallowing, neck rotation, and secondary visual loss.

We selected the operative procedure and need of joint fixation on the basis of the morphometric analyses performed during craniocervical traction test. This strategy improved or stabilized the neurological symptoms and/or bony fusion in CCF. In children aged younger than 12 years with instability of CCJ in CM-I type A, CCF surgery should be delayed until the patient is 12 years old or the development is complete.

Conclusions

Morphometric analyses of PCF and CCJ should be performed to determine the mechanism and treatment of ptosis of the brainstem and cerebellum. CM-I was divided into three independent types by morphometric analysis.

Surgical treatment of CM-I was selected based on the mechanism of ptosis of the brainstem and cerebellum in each CM-I type. All surgical treatments had good outcome and safety profile. The appropriate surgical method for the management of CM-I should address the mechanism underlying ptosis of the brainstem and cerebellum. It is important to confirm the normalization of CSF flow during the operation.

In this study, FMD was initially performed for patients younger than 12 years. Patients younger than 12 years with CM-I types A and C should be monitored for persistent syringomyelia and deterioration of neurological symptoms/signs. In such cases, additional surgery with ESCP or CCJ should be performed after the age of 12 years.

Morphometric analyses of CCJ during craniocervical traction test should be performed to identify the instability of joints and decide the appropriate operative procedure for fixation. CCF achieved high rate of improvement of neurological symptoms and joint stabilization.

Acknowledgments

The authors thank Professor Emeritus Thomas H. Milhorat, M.D., Feinstein Institute of Neurosciences, Northwell Health, Manhasset, New York.

Abbreviations

ADI = distance between the anterior arch of the atlas and dens

AXA = angle between the axis and atlas

BAI = distance between the plane of the posterior surface of the anterior arch of the atlas and basion

BDI = distance between the basion and the top of dens

CM-I = Chiari malformation type I

CM-II = Chiari malformation type II

CCF = craniocervical fixation

CCJ = craniocervical junction

CXA = angle between the plane of clivus and plane of dens

C1/2 FIX = atlanto-axial posterior lateral fixation

DAI = vertical distance between the top part of dens and the lowest line of the axis

ESCP = expansive suboccipital cranioplasty

FMD = foramen magnum decompression

HDCT = hereditary disorders of connective tissue

JOA = Japanese Orthopaedic Association

OCF = occipito-cervical posterior lateral fixation

PCF = posterior cranial fossa

VAFM = volume of the area surrounding the foramen

magnum

VBPCF = volume of brain in PCF

VPCF = volume of posterior cranial fossa

Ethics

This report was approved by the Institutional Review Board of Memorial Moriguchi-Ikuno Hospital and Osaka Metropolitan University Graduate School of Medicine.

Informed Consent

Informed consent was obtained from all patients, normal volunteers, and relevant persons.

Conflicts of Interest Disclosure

The authors report no conflict of interest relevant to this research. All authors, who are members of the Japanese Neurological Society (JNS), and Paolo A. Bolgnese, who is a member of the American Association of Neurological Surgeons (AANS), have completed the online self-reported COI disclosure statement form through the website of JNS or AANS.

References

- Nishikawa M, Sakamoto H, Hakuba A, Nakanishi N, Inoue Y: Pathogenesis of Chiari malformation: a morphometric study of the posterior cranial fossa. *J Neurosurg* 86: 40-47, 1997
- Milhorat TH, Chou MW, Trindal EM, Mandell M, Wolpert C, Speer CA: Chiari I malformation redefined: clinical and radiographic findings for 364 symptomatic patients. *Neurosurgery* 44: 1005-1017, 1999
- Milhorat TH, Nishikawa M, Kula WR, Dlugacz DY: Mechanisms of cerebellar tonsil herniation in patients with Chiari malformations as guide to clinical management. *Acta Neurochir* 152: 1117-1127, 2010
- Stovner LJ, Bergan U, Nilsen G, Sjaastad O: Posterior cranial fossa dimensions in the Chiari I malformation: relation to pathogenesis and clinical presentations. *Neuroradiology* 55: 113-118, 1993
- Sakamoto H, Nishikawa M, Nakanishi N, Hakuba A, Tokuno H: [Surgical treatment of syringomyelia associated with Chiari malformation]. *Spine Surgery* 8: 1-6, 1994 (Japanese)
- Badie B, Mendoza D, Batzdorf U: Posterior cranial fossa volume and response to suboccipital decompression in patients with Chiari I malformation. *Neurosurgery* 37: 214-218, 1995
- Karagoz F, Izgi N, Sencer SK, et al.: Morphometric measurements of the cranium in patients with Chiari type I malformation and comparison with the normal population. *Acta Neurochir* 144: 165-171, 2012
- Alperin N, Loftus JR, Oliu CJ, et al.: Magnetic resonance imaging measures of posterior cranial fossa morphology and cerebrospinal fluid physiology in Chiari malformation type I. *Neurosurgery* 75: 515-522, 2014
- Speer MC, Gerge TM, Enterline DS, et al.: A genetic hypothesis for Chiari I malformation with or without syringomyelia. *Neurosurg Focus* 8: E121, 2000
- Fischl B, Salat DH, Busa E: Whole brain segmentation labeling of neuroanatomical structures in the human brain. *Neuron* 33: 341-355, 2002
- Nishikawa M: [Chiari malformation and its related disorders—embryology, pathogenesis, classification and strategy of surgical treatment]. *Spine Surgery* 35: 142-150, 2021 (Japanese)
- Milhorat TH, Bolognese PA, Nishikawa M, McDonnell NB, Francomano CA: Syndrome of occipitoatlantoaxial hypermobility, functional cranial settling and Chiari malformation I patients with hereditary disorders of connective tissue. *J Neurosurg Spine* 7: 601-609, 2007
- Milhorat TH, Bolognese PA, Nishikawa M, et al.: Association of Chiari malformation type I and tethered cord syndrome: preliminary results of section filum terminale. *Surg Neurol* 71: 20-35, 2009
- DaoTring P, Beynon C, Unterberg A, Schneider T, Jesser J: Racial differences in the anatomy of the posterior cranial fossa: neurosurgical considerations. *World Neurosurg* 117: e571-e574, 2018
- Zhang Y, Scheparts LA: Three-dimensional geometric morphometric study of modern human occipital variation. *PLoS One* 14: e0245445, 2021
- Goel A, Gore S, Shah A, Dharukar P, Vutha R, Patil A: Atlantoaxial fixation for Chiari I formation in pediatric age group patients: report of treatment in 33 patients. *World Neurosurg* 111: e668-e677, 2018
- Ranawat CS, O'Leary P, Pellicci P, et al.: Cervical spine fusion in rheumatoid arthritis. *J Bone Joint Surg Am* 61: 1003-1010, 1979
- Harris JH Jr, Carson GC, Wagner LK: Radiologic diagnosis of traumatic occipitovertebral dissociation: 1. Normal occipitovertebral relationships on lateral radiographs of supine subjects. *AJR Am J Roentgenol* 162: 881-886, 1994
- Harris JH Jr, Carson GC, Wagner LK, et al.: Radiologic diagnosis of traumatic occipitovertebral dissociation: 2. Comparison of three methods of detecting occipitovertebral relationships on lateral radiographs of supine subjects. *AJR Am J Roentgenol* 162: 887-892, 1994
- Smoker WR: Craniovertebral junction: normal anatomy, craniometry, and congenital anomalies. *Radiographics* 14: 255-277, 1994
- Hoyte DAN: Growth of the cranial base in human, in Dexon AD, Hoyte DAN, Ronning O (eds): *Fundamentals of Craniofacial Growth*. New York, CRC Press, 1997, pp 278-291
- Sgouros S, Kountouri M, Natarajan K: Posterior fossa volume in child with Chiari malformation type I. *J Neurosurg* 105: 101-106, 2006
- Fukuoka T, Nishimura Y, Hara M, et al.: Chair type I malformation-induced intracranial hypertension with diffuse brain edema treated with foramen magnum decompression: a case report. *NMC Case Report J* 12: 115-120, 2017
- Taylor DG, Mastorakos P, Jane JA Jr, Oldfield EH: Two distinct populations of Chiari I malformation based on presence or absence of posterior cranial fossa crowdedness on magnetic resonance imaging. *J Neurosurg* 129: 1934-1940, 2017
- Muller F, O'Rahilly R: The human chondrocranium at the end of the embryonic period proper with particular reference to the nervous system. *Am J Anat* 159: 33-58, 1980
- O'Rahilly R, Muller F, Meyer DB: The human vertebral column at the end of the embryonic period proper. The occipito-cervical region. *J Anat* 136: 181-195, 1983
- Geddes DM, Cargill RS, LaPlaca MC: Mechanical stretch in neurons results in a strain rate and magnitude-dependent increasing

- in plasma membrane permeability. *J Neurotrauma Rev* 20: 1039-1049, 2003
- 28) Nishikawa M, Bolognese PA, Kula RW, Ikuno H, Ohata K: Pathogenesis and classification of Chiari malformation type I based on the mechanism of ptosis of the brain stem and cerebellum: a morphometric study of the posterior cranial fossa and craniovertebral junction. *J Neurol Surg B* 82: 277-284, 2021
- 29) Nishikawa M, Bolognese PA, Kula RW, Ikuno H, Takami T, Ohata K: Surgical management of Chiari malformation: preliminary results of surgeries for mechanisms of ptosis of the brain stem and cerebellum. *J Neurol Surg B* 82: 264-272, 2021
- 30) Oaks J: Chiari malformation and syringomyelia, in Reagachary SS, Williams RH (eds): Principles of Neurosurgery. London, Mosby-Wolf, 1994, pp 9.1.189
- 31) Nishikawa M, Ohata K: [Operation of Chiari malformation], in Ohata K (ed): Spinal Surgery, Neurosurgery Now. Tokyo, Medical View, 2011, pp 138-153 (Japanese)
- 32) Sakamoto H, Nishikawa M, Hakuba A, Tokunou N, Nakanishi N, Nishimura S: Expansive suboccipital cranioplasty for the treatment of syringomyelia associated with Chiari malformation. *Acta Neurochir* 123: 949-961, 1999
- 33) Hirabayashi K: [Japanese Orthopaedic Association score in cervical spondylotic myelopathy]. *Nippon Seikeigekagakkai Zasshi* 68: 490-503, 1994 (Japanese)
- 34) Milhorat TH, Bolognese PA: Tailored operative technique for Chiari type I malformation using intraoperative color Doppler ultrasonography. *Neurosurgery* 53: 890-905, 2003
- 35) Winegar CD, Lawrence JP, Friel BC, et al.: A systemic review of occipital cervical fusion: technique and outcome. *J Neurosurg Spine* 13: 5-16, 2010
- 36) Nishikawa M, Milhorat TH, Bolognese PA, Kula RW, Masamura S, Ikuno H: Fusion in patients with occipito-atlanto-axial joint instability-management strategy and results. *Spinal Surgery* 26: 211-220, 2012 (Japanese)
- 37) Nishikawa M, Ohata K, Baba M, et al.: Chiari I malformation associated with ventral compression and instability: one staged posterior decompression and fusion with a new instrumentation technique. *Neurosurgery* 54: 193-196, 2004
- 38) Batzdorf U, McArthur DL, Bentson JR: Surgical treatment of Chiari malformation with and without syringomyelia: experience with 177 adult patients. *J Neurosurg* 118: 232-242, 2013
- 39) Klekamp J, Batzdorf U, Samii M, Bothe HW: The surgical treatment of Chiari malformation. *Acta Neurochir* 138: 788-801, 1996
- 40) Tubbs RS, Beckman J, Naftel RP, Chern JJ, Wellons JC III, Rozzele CJ: Institutional experience with 500 cases of pediatric patients with Chiari malformations. *J Neurosurg Pediatr* 7: 248-256, 2011
- 41) Bhimani A, Chiu RG, Esfahani DR, et al.: C1-2 fusion versus occipito-cervical fusion for high cervical fractures: a multi-institutional database analysis and review of the literature. *World Neurosurg* 119: e456-e459, 2018

Corresponding author: Misao Nishikawa, M.D., Ph.D.

Department of Neurosurgery, Moriguchi-Ikuno Memorial Hospital, 6-17-33 Satanakamachi, Moriguchi City, Osaka 570-0002, Japan.

e-mail: misaonishikawa88@gmail.com